

This discussion paper is/has been under review for the journal *Climate of the Past* (CP).
Please refer to the corresponding final paper in CP if available.

The challenge of simulating warmth of the mid-Miocene Climate Optimum in CESM1

A. Goldner¹, N. Herold¹, and M. Huber^{1,2}

¹Earth, Atmospheric, and Planetary Sciences, Purdue University, 550 Stadium Mall Drive, West Lafayette, IN 47907, USA

²Purdue Climate Change Research Center, Purdue University, Mann Hall 203 S. Martin Jischke Drive, West Lafayette, IN 47907, USA

Received: 10 June 2013 – Accepted: 18 June 2013 – Published: 26 June 2013

Correspondence to: A. Goldner (agoldner@purdue.edu)

Published by Copernicus Publications on behalf of the European Geosciences Union.

CPD

9, 3489–3518, 2013

Simulating warmth of the mid-Miocene Climate Optimum in CESM1

A. Goldner et al.

Title Page

Abstract

Introduction

Conclusions

References

Tables

Figures

⏪

⏩

◀

▶

Back

Close

Full Screen / Esc

Printer-friendly Version

Interactive Discussion

al., 2008; Shevenell et al., 2008). These warm extra-tropical temperatures have been hard to reconcile with reconstructed below-modern tropical sea surface temperature (SST) records and boron and alkenone CO₂ reconstructions of 200–280 ppm levels (Pagani et al., 2005; Pearson and Palmer, 2000).

Recent re-evaluation of the proxy records has led to advancement in our understanding of MMCO warmth. First, the MMCO tropical SST records showing below-modern levels (Savin, 1977; Nikolaev et al., 1998; Bojar et al., 2005) are now understood to have a cool diagenetic bias (Stewart et al., 2004). Excluding these records indicates that tropical SSTs in the Miocene were above modern (Shevenell et al., 2004; You et al., 2009; LaRiviere et al., 2012). Second, recent leaf stomatal studies reconstruct CO₂ concentrations at the MMCO to be 400–500 ppm (Kürschner et al., 2008) and these results have been confirmed in boron isotope-based reconstructions (Foster et al., 2012) and updated alkenone reconstructions (Zhang et al., 2013).

Nevertheless, even with higher CO₂ concentrations MMCO warming has been difficult to reproduce in an intermediate complexity Earth system model (Henrot et al., 2010), atmosphere and slab ocean models (Tong et al., 2009; You et al., 2009), and fully coupled atmosphere ocean models (Herold et al., 2011; Krapp and Jungclaus, 2011). For example, Herold et al. (2011) found that the Community Climate System Model (CCSM3.0) was ~10°C too cold compared to proxy records in high latitude regions like Alaska and Antarctica. In this study, we implement boundary conditions from Herold et al. (2011) within the National Center for Atmospheric Research (NCAR) Community Earth System Model (CESM1.0) using the Community Atmosphere Model (CAM4) framework to simulate the MMCO. This allows for a clean comparison with previous simulations done with CCSM3.0, using a latest generation model included in the Coupled Model Intercomparison Project (CMIP5).

To explore if the modelling framework is able to match MMCO warmth we conduct a pointwise model data comparison using proxy records compiled for the MMCO (Tables S1 and S2). The MMCO is a good choice for climate model validation because the continental configuration is relatively close to modern (Herold et al., 2008) although

CPD

9, 3489–3518, 2013

Simulating warmth of the mid-Miocene Climate Optimum in CESM1

A. Goldner et al.

[Title Page](#)

[Abstract](#)

[Introduction](#)

[Conclusions](#)

[References](#)

[Tables](#)

[Figures](#)

[⏪](#)

[⏩](#)

[◀](#)

[▶](#)

[Back](#)

[Close](#)

[Full Screen / Esc](#)

[Printer-friendly Version](#)

[Interactive Discussion](#)



Simulating warmth of the mid-Miocene Climate Optimum in CESM1

A. Goldner et al.

[Title Page](#)

[Abstract](#)

[Introduction](#)

[Conclusions](#)

[References](#)

[Tables](#)

[Figures](#)

[⏪](#)

[⏩](#)

[◀](#)

[▶](#)

[Back](#)

[Close](#)

[Full Screen / Esc](#)

[Printer-friendly Version](#)

[Interactive Discussion](#)



differences exist (Potter and Szatmari, 2009). Additionally, the CO₂ levels during the MMCO are in the range of values for the next century, and paleoclimate records are better constrained compared to earlier warm periods such as the Eocene (~ 56–33.9 Ma) where there is large uncertainty in the CO₂ (Pagani, 2002; Pearson and Palmer, 2000; Royer et al., 2012) and temperature records.

2 Methods

2.1 Modelling framework

A series of MMCO global climate simulations are conducted using components of the NCAR CESM1.0 (Gent et al., 2011). The Community Atmospheric Model (CAM4) is run at 1.9° × 2.5° horizontal resolution with 26 vertical levels and coupled to the Community Land Model (CLM4) (Lawrence et al., 2012), the Community Sea-Ice Model (CICE4) (Hunke and Lipscomb, 2008) and the slab ocean model, described below (Bitz et al., 2012). This model simulates modern surface temperature distributions and equator to pole temperature gradients well (Gent et al., 2011), although biases exist (Kay et al., 2012; Neale et al., 2013).

2.2 Experimental design

The control Pre-industrial (PI) simulation employs the modelling components described above in standard configuration and with CO₂ concentrations set at 287 ppm. The slab ocean forcing file for the PI case has heat fluxes, salinity, and density inputs from a fully coupled atmosphere, ocean, ice, and land simulation (Bitz et al., 2012). Additionally we run a PI simulation at 400 ppm CO₂ (PI400) to compare with our MMCO simulation (also at 400 ppm CO₂). This high CO₂ PI configuration allows us to isolate the temperature effect of including MMCO boundary conditions at constant CO₂.

The MMCO simulation has vegetation cover and topography described in Herold et al. (2011). Previous slab ocean and atmosphere MMCO simulations have been con-

and S2). We present the longitudinal and spatial distribution of the proxy records in Fig. 1. The proxy reconstruction spans over the MMCO (17–14.50 Ma), however, because of the sparseness of data over this period we include records that have an average age between 20 and 13.65 Ma, where they fill spatial gaps (i.e. Southern Hemisphere). This data compilation can be used as a reference data set for future MMCO model data comparisons.

We update the minimum error in our compiled terrestrial proxy records for a number of reasons. Firstly, recent work suggests that for physiognomic leaf-climate methods there should be a minimum error of $\pm 5^\circ\text{C}$ (Royer, 2012). Secondly, studies have suggested that there is large uncertainty in estimating MAT (Grimm and Denk, 2012) using the coexistence approach (Mosbrugger and Utescher, 2007). For our intended purposes increasing the minimum proxy record uncertainty should make matching the simulations more obtainable. If our model still fails to match proxy data even with generous error bars this merely proves our main results further.

The SST records are compiled from available published data in the literature and we describe these records in detail in Table S2. We leave out some tropical SST records which may have a diagenetic bias as described in (Sexton et al., 2006; Huber, 2008). Tropical SSTs are few and far between for the MMCO, but more common in the mid-to-late Miocene, thus we may omit proxy records from over almost half the surface area of the planet (30°N and 30°S) or utilize data from intervals slightly outside the MMCO. Because there is a lack of tropical SST data points for the MMCO we compile SSTs from the late Miocene and justify this based off the minimal change between middle and late Miocene SSTs at other locations (LaRiviere et al., 2012). Given that the Pliocene tropical SSTs were $\sim 4\text{--}6^\circ\text{C}$ (Brierley et al., 2009; Dekens et al., 2007; Ravelo et al., 2006; Fedorov et al., 2013) above modern and the late Miocene were $\sim 7\text{--}9^\circ\text{C}$ above modern (LaRiviere et al., 2012) it is reasonable to conjecture MMCO tropical SSTs were this warm or warmer. Either approach introduces potential errors in interpretation and here we choose to utilize SST estimates in data sparse regions that lie generally within the early to middle Miocene, but may be outside the MMCO. Our

Simulating warmth of the mid-Miocene Climate Optimum in CESM1

A. Goldner et al.

Title Page

Abstract

Introduction

Conclusions

References

Tables

Figures



Back

Close

Full Screen / Esc

Printer-friendly Version

Interactive Discussion



updated minimum error bars are large enough to encompass the temporal variation in these records.

Previous work has discussed the importance of including orbital variations when quantifying uncertainty in model data comparisons (Haywood et al., 2013). To quantify the possible error introduced by aliasing of orbital variability in our interpretation of model data mismatch, we conduct two sensitivity experiments varying obliquity to minimum and maximum Miocene values (22° and 25° respectively). We then calculate the maximum and minimum model-derived temperatures at each proxy location from both extreme orbit simulations and use this absolute anomaly as an estimate of orbitally induced variance. These maximum and minimum values are plotted as vertical error bars on the modelled MAT in our pointwise model data comparisons (Figs. 2, 3, 4, 5, 6).

3 Results

3.1 Proxy derived MAT value

To determine the difference in global MAT between Miocene and pre-industrial climate we take the proxy records and perform a pointwise anomaly of proxy-derived MAT compared to modern observed MAT at paleo-latitudes and paleo-longitudes. We split the resulting anomalies into tropical (30° N to 30° S) mid-latitude (30° N/S to 60° N/S) and polar (60° N/S to 90° N/S) regions and conduct a weighted average anomaly over each latitudinal region. This latitudinal binning and area weighting addresses issues of having more proxy records in certain regions (i.e. the mid-latitudes). Using proxy records for the MMCO (Table S1 and S2) we calculate a global MAT change of $\sim 7.6^\circ\text{C} \pm 2.30$ (We report two standard errors from the mean) compared to PI. The proxy-derived temperatures compared against modern observations (ECMWF 40 Year Reanalysis Project) is $6.8^\circ\text{C} \pm 2.20$ as there is $\sim 1.0^\circ\text{C}$ of warming between modern observations and PI climate.

Simulating warmth of the mid-Miocene Climate Optimum in CESM1

A. Goldner et al.

Title Page

Abstract

Introduction

Conclusions

References

Tables

Figures

⏪

⏩

◀

▶

Back

Close

Full Screen / Esc

Printer-friendly Version

Interactive Discussion



Simulating warmth of the mid-Miocene Climate Optimum in CESM1

A. Goldner et al.

[Title Page](#)

[Abstract](#)

[Introduction](#)

[Conclusions](#)

[References](#)

[Tables](#)

[Figures](#)

[⏪](#)

[⏩](#)

[◀](#)

[▶](#)

[Back](#)

[Close](#)

[Full Screen / Esc](#)

[Printer-friendly Version](#)

[Interactive Discussion](#)



To validate our approach for estimating proxy derived MAT we calculate a resampled MAT using our methodology and compare against a globally weighted MAT (we will call this true MAT) from both model runs and modern observational datasets. The globally weighted true MAT value of the MMCO simulation is 18.00 °C (Table 1) whereas our calculation for MAT resampled over the proxy record regions using the methodology from above is 17.12 °C. The calculated standard error from the mean including proxy record uncertainty is 1.33 °C, which illustrates that our resampled MAT value is well within the calculated standard error. We also calculate the resampled MAT using modern observations and with other Miocene simulations and find that all the resampled MAT estimates fall within two standard errors of the true MAT. For all intended purposes we are confident that our approach for reconstructing global MAT from our proxy record compilation is a valid estimate.

3.2 MMCO simulation compared against the proxy records

The MMCO simulation is 4.04 °C warmer than the control PI simulation, but the simulation is about 4 °C cooler than globally averaged MMCO proxy temperature reconstructions (Table 1). The MMCO simulation generally captures the tropical and mid-latitude temperature distribution of the proxy records, but fails to achieve above-freezing temperatures in the high latitudes (Fig. 2b, Table 2). The nature of this discrepancy can be clarified by examining the equator to pole surface temperature gradient. It is 17 °C larger in the MMCO simulation than in the proxy records (Table 1). Using the methods described in Lunt et al. (2012), the equator to pole temperature gradient is calculated by averaging the mean annual temperatures over the absolute latitudes of (60–80° minus (0–30°); except here we use 80° because this the maximum latitudinal extent of proxy records. Additionally, an error weighted best fit line for the pointwise comparison reveals a root mean square (RMS) error of ~6 °C and y-intercept of –6 °C, although the slope of the regression line is close to 1 (Table 1). In summary, the MMCO simulation (at 400 ppm CO₂) is unable to produce high latitude warmth or a sufficiently warm global mean temperature compared to the paleo temperature records.

3.3 Effect of MMCO boundary conditions and CO₂ sensitivity experiments

We find that our MMCO simulation is 2.43 °C warmer compared to the PI simulation run at 400 ppm CO₂ (PI400). Thus 2.43 °C of the temperature difference between our MMCO and PI simulations are a result of changes in continental positions, topography, and vegetation. This change is consistent with late Miocene modelling which finds 3.0 °C of warming due to changes in vegetation and topography (Knorr et al., 2011).

A CO₂ sensitivity experiment run at 560 ppm CO₂ (above most reconstructed CO₂ records) is also too cold at high latitudes compared to proxy records (Fig. 3b) and the equator to pole temperature difference is still too large by ~ 13 °C (Table 1). This simulation has a global MAT 5.89 °C higher than the control PI simulation, and is ~ 2 °C colder than the proxy-derived global MAT. The error weighted best fit line for the MMCO560 pointwise comparison gives a y-intercept of ~ -2.5 °C, but the calculated RMS error is still 5.7 °C (Table 1). The MMCO800 simulation has a MAT 7.26 °C above PI (Table 1), which is our best comparison with the proxy derived MAT value. The error weighted best fit line is also very close to the one to one line and has a y-intercept close to zero (Fig. 3d). Overall MMCO800 matches the proxy compilation the best and we use this comparison to prove that matching global MMCO warmth can be accomplished, but at CO₂ concentrations approximately twice that reconstructed from proxies. These results are very similar to those found in the Eocene (Huber and Caballero, 2011; Lunt et al., 2012)

Below, we test hypotheses that have been proposed to explain Miocene warmth, with the goal of improving the model data comparison without having to increase CO₂ above reconstructed levels.

Simulating warmth of the mid-Miocene Climate Optimum in CESM1

A. Goldner et al.

[Title Page](#)

[Abstract](#)

[Introduction](#)

[Conclusions](#)

[References](#)

[Tables](#)

[Figures](#)

[⏪](#)

[⏩](#)

[◀](#)

[▶](#)

[Back](#)

[Close](#)

[Full Screen / Esc](#)

[Printer-friendly Version](#)

[Interactive Discussion](#)



4 Further sensitivity studies

4.1 Reducing Antarctic ice-sheet volume

Recent work estimates the volume of the middle Miocene Antarctic Ice Sheet (AIS) to be $\sim 30\text{--}50\%$ less than modern (Shevenell et al., 2008). Consequently the Herold et al. (2008) reconstruction for AIS elevation and extent is likely too large (Fig. 2a). To correct this, we utilize a new AIS reconstruction derived from a fully interactive terrestrial ice and atmosphere model (Pollard personal communication) (Fig. 4a). We introduce an AIS that is half the volume of that used in Herold et al. (2011) (Fig. 2a) from the offline interactive ice sheet simulation. This new AIS volume is within the range of estimates from proxy records (Pekar and DeConto, 2006; Billups and Schrag, 2003). We also reduce the area of glacier albedo over Antarctica by half and replace it with a combination of unvegetated and tundra-like land cover. We introduce this new AIS topography and vegetation cover (Fig. 4a) into the MMCO boundary conditions described in Herold et al. (2008) and denote this simulation LOW AIS. The difference in surface albedo over the AIS between these two simulations ends up being similar as snow (also with a high albedo) ends up covering the areas that were once glacier because Antarctica stays below freezing year round.

The LOW AIS simulation is 4.15°C warmer than PI and 0.10°C warmer than the previously described MMCO simulation with a high AIS (Fig. 4c). Thus, there is no significant global mean temperature impact from decreasing the size of the AIS, consistent with previous work (Goldner et al., 2013). Although recent coupled MMCO simulations have found warmer and wetter conditions regionally over Europe due to reducing ice extent in Antarctica highlighting the importance of including ocean feedbacks for resolving regional temperature distributions (Hamon et al., 2012). The temperature difference between LOW AIS and the MMCO simulation is largest over Antarctica (Fig. 4b) because of the imposed elevation and surface albedo changes. Although lowering the AIS warms the Antarctic continent, the Miocene LOW AIS simulation results in negligible improvement in matching proxy records elsewhere in the high latitudes (Table 2).

Simulating warmth of the mid-Miocene Climate Optimum in CESM1

A. Goldner et al.

Title Page

Abstract

Introduction

Conclusions

References

Tables

Figures

⏪

⏩

◀

▶

Back

Close

Full Screen / Esc

Printer-friendly Version

Interactive Discussion



Simulating warmth of the mid-Miocene Climate Optimum in CESM1

A. Goldner et al.

[Title Page](#)

[Abstract](#)

[Introduction](#)

[Conclusions](#)

[References](#)

[Tables](#)

[Figures](#)

[⏪](#)

[⏩](#)

[◀](#)

[▶](#)

[Back](#)

[Close](#)

[Full Screen / Esc](#)

[Printer-friendly Version](#)

[Interactive Discussion](#)

In the EP simulation, high latitude regions warm, especially Alaska and Antarctica (Fig. 5a). The pointwise model data comparison for the EP simulation is plotted in Fig. 5b. This simulation is $\sim 4.6^\circ\text{C}$ warmer in global mean than the PI simulation and $\sim 0.5^\circ\text{C}$ warmer than the MMCO and LOW AIS simulations. Warming due to adding El Padre is largest in regions where the model previously performed the worst (Fig. 5a). Roughly 2°C of warming occurs in Alaska, but the simulation is still $\sim 8.5^\circ\text{C}$ too cold in this region (Table 2) and still has a $\sim 13^\circ\text{C}$ larger equator to pole surface temperature gradient compared to the proxy records (Table 1). Imposing an El Padre illustrates a mechanism capable of warming the high latitudes without elevating CO_2 consistent with the results of (LaRiviere et al., 2012; Sriver and Huber, 2010; Brierley et al., 2009). Nevertheless this change does not reconcile the warmth of the MMCO, as temperatures are still $\sim 2^\circ\text{C}$ too cool globally and $\sim 8.5^\circ\text{C}$ too cool in the high latitudes.

Adding EP and increasing obliquity to 25° results in a simulation that is 5.64°C warmer than PI (Fig. 6). This MAT anomaly compared to PI is similar to the warming found in the MMCO560 simulation. The MMCO560 simulation does not include any of the boundary condition changes aimed at increasing high latitude warmth. Interestingly the EP, AIS, and obliquity forcing results in a 4°C improvement in simulating the equator to pole temperature gradient compared to MMCO560 (Table 1). Both comparisons are too cold compared to the proxy derived global MAT value as matching the proxy records in high latitudes requires a CO_2 concentration double what is predicted in the reconstructions.

5 Discussion

5.1 Comparison with previous MMCO CCSM3.0 simulations

The most comparative study to the experiments presented here are the CCSM3.0 MMCO simulations described in Herold et al. (2011) (Table 1). The CESM1.0 Miocene simulations are $\sim 2.0^\circ\text{C}$ warmer than the Miocene CCSM3.0 simulations (Herold et

bles S1 and S2) we are confident in the broad trends reflected in the proxy record. Thus, explaining the warming will require additional incremental changes in boundary conditions (such as an even higher CO₂), a more sensitive model to background CO₂ concentrations, and/or identification of some – as yet unknown – process or forcing that accounts for almost half of the difference in temperature between today and the MMCO.

Although some terrestrial CO₂ proxies suggest CO₂ was higher than 500 ppm, this would not solve the data model mismatch, as increasing CO₂ past 560 would likely make the tropics too warm (e.g. Fig. 3b, d). Ultimately, our inability either to identify a missing paleoclimate forcing or formulate models with sufficient positive feedbacks to recreate substantial increases in global mean temperature with strong polar amplification represents a persistent weakness of climate models.

Supplementary material related to this article is available online at:
<http://www.clim-past-discuss.net/9/3489/2013/cpd-9-3489-2013-supplement.pdf>.

Acknowledgements. We acknowledge support of the Computational Sciences and Engineering (CS&E) program which supports the first author through a GAANN fellowship. The authors would like to thank Christine Shields and David Pollard who helped with some of the implementation and development of the Miocene simulations. We also thank Matthew Pound who supplied us with his middle Miocene terrestrial data compilation. In addition, parts of this research were funded by an NSF P2C2 grant 0902882 and NSF EAR grant 1049921. This is PCCRC paper 1301.

Simulating warmth of the mid-Miocene Climate Optimum in CESM1

A. Goldner et al.

Title Page

Abstract

Introduction

Conclusions

References

Tables

Figures



Back

Close

Full Screen / Esc

Printer-friendly Version

Interactive Discussion



References

- Barreiro, M., Philander, G., Pacanowski, R., and Fedorov, A.: Simulations of warm tropical conditions with application to middle Pliocene atmospheres, *Clim. Dynam.*, 26, 349–365, doi:10.1007/s00382-005-0086-4, 2006. 3499
- 5 Billups, K. and Schrag, D. P.: Application of benthic foraminiferal Mg/Ca ratios to questions of Cenozoic climate change, *Earth Planet. Sci. Lett.*, 209, 181–195, doi:10.1016/S0012-821X(03)00067-0, 2003. 3498
- Bitz, C. M., Shell, K. M., Gent, P. R., Bailey, D., Danabasoglu, G., Armour, K. C., Holland, M. M., and Kiehl, J. T.: Climate sensitivity of the community climate system model version 4, *J. Climate*, 25, 3053–3070, doi:10.1175/JCLI-D-11-00290.1, 2012. 3492, 3493
- 10 Böhme, M., Bruch, A. A., and Selmeier, A.: The reconstruction of Early and Middle Miocene climate and vegetation in Southern Germany as determined from the fossil wood flora, *Palaeogeogr. Palaeocli.*, 253, 91–114, doi:10.1016/j.palaeo.2007.03.035, 2007. 3490
- Bonham, S., Haywood, A., Lunt, D., Collins, M., and Salzmann, U.: El Niño-Southern Oscillation, Pliocene climate and equifinality, *Philos. T. Royal Soc. A.*, 367, 127–156, doi:10.1098/rsta.2008.0212, 2009. 3499
- 15 Bojar, A. V., Hiden, H., Fenninger, A., and Neubauer, F.: Middle Miocene temperature changes in the central paratethys: Relations with the East Antarctica ice sheet development, paper presented at South American Symposium on Isotope Geology, Dep. of Geol., Fed. Univ. of Pernambuco, Salvador, Brazil, 2005. 3491
- 20 Brierley, C. M., Fedorov, A. V., Lui, Z., Herbert, T., Lawrence, K., and LaRiviere, J. P.: Greatly expanded tropical warm pool and weakened Hadley circulation in the early Pliocene, *Science*, 323, 1714–1718, doi:10.1126/science.1167625, 2009. 3494, 3500
- Danabasoglu, G., Bates, S. C., Briegleb, B. P., Jayne, S. R., Jochum, M., Large, W. G., and Yeager, S. G.: The CCSM4 ocean component, *J. Climate*, 25, 1361–1389, 2012. 3493
- 25 Dekens, P. S., Ravelo, A. C., and McCarthy, M. D.: Warm upwelling regions in the Pliocene warm period, *Paleoceanography*, 22, PA3211, doi:10.1029/2006PA001394, 2007. 3494
- Fedorov, A. V., Brierley, C. M., Lawrence, K. T., Liu, Z., Dekens, P. S., and Ravelo, A. C.: Patterns and mechanisms of early Pliocene warmth, *Nature*, 496, 43–49, doi:10.1038/nature12003, 30 2013. 3494

Simulating warmth of the mid-Miocene Climate Optimum in CESM1

A. Goldner et al.

[Title Page](#)

[Abstract](#)

[Introduction](#)

[Conclusions](#)

[References](#)

[Tables](#)

[Figures](#)

[⏪](#)

[⏩](#)

[◀](#)

[▶](#)

[Back](#)

[Close](#)

[Full Screen / Esc](#)

[Printer-friendly Version](#)

[Interactive Discussion](#)



Simulating warmth of the mid-Miocene Climate Optimum in CESM1

A. Goldner et al.

[Title Page](#)
[Abstract](#)
[Introduction](#)
[Conclusions](#)
[References](#)
[Tables](#)
[Figures](#)




[Back](#)
[Close](#)
[Full Screen / Esc](#)
[Printer-friendly Version](#)
[Interactive Discussion](#)

- Foster, G. L., Lear, C. H., and Rae, J. W. B.: The evolution of pCO₂, ice volume and climate during the Middle Miocene, *Earth Planet Sci. Lett.*, 341–344, 243–254, doi.org/10.1016/j.epsl.2012.06.007, 2012. 3491
- Galeotti, S., von der Heydt, A., Huber, M., Bice, D., Dijkstra, H., Jilbert, T., and Reichert, G. J.: Evidence for active El Niño Southern Oscillation variability in the Late Miocene greenhouse climate, *Geology*, 38, 419–422, doi: 10.1130/G30629.1, 2010. 3499
- Gent, P. R., Danabasoglu, G., Donner, L. J., Holland, M. M., Hunke, E. C., Jayne, S. R., Lawrence, D. M., Neale, R. B., Rasch, P. J., Vertenstein, M., Worley, P. H., Yang, Z.-L., and Zhang, M.: The Community Climate System Model version 4, *J. Climate*, 24, 4973–4991, doi:10.1175/2011JCLI4083.1, 2012. 3492
- Gettelman, A., Kay, J. E., and Shell, K. M.: The evolution of climate sensitivity and climate feedbacks in the Community Atmosphere Model, *J. Climate*, 25, 1453–1469, doi:10.1175/JCLI-D-11-00197.1, 2012. 3493, 3501
- Goldner, A., Huber, M., Diffenbaugh, N., and Caballero, R.: Permanent El Niño teleconnection “blueprint” for past global and North American hydroclimatology, *Clim. Past*, 7, 723–743, doi:10.5194/cp-7-723-2011, 2011. 3499
- Goldner, A., Huber, M., and Caballero, R.: Does Antarctic glaciation cool the world?, *Clim. Past*, 9, 173–189, doi:10.5194/cp-9-173-2013, 2013 3498
- Grimm, G. W. and Denk, T.: Reliability and Resolution – a revalidation of the co-existence approach using modern-day data, *Rev. Palaeobot. Palynol.*, 172, 33–47, doi:10.1016/j.revpalbo.2012.01.006, 2012. 3494
- Hamon, N., Sepulchre, P., Donnadiou, Y., Henrot, A. J., François, L., Jaeger, J. J., and Ramstein, G.: Growth of subtropical forests in Miocene Europe: The roles of carbon dioxide and Antarctic ice volume, *Geology*, 40, 567–570, doi:10.1130/G32990.1, 2012. 3498
- Haywood, A. M., Valdes, P. J., and Peck, V. L.: A permanent El Niño-like state during the Pliocene?, *Paleoceanography*, 22, PA1213, doi:10.1029/2006PA001323, 2007. 3499
- Haywood, A. M., Hill, D. J., Dolan, A. M., Otto-Bliesner, B. L., Bragg, F., Chan, W.-L., Chandler, M. A., Contoux, C., Dowsett, H. J., Jost, A., Kamae, Y., Lohmann, G., Lunt, D. J., Abe-Ouchi, A., Pickering, S. J., Ramstein, G., Rosenbloom, N. A., Salzmann, U., Sohl, L., Stepanek, C., Ueda, H., Yan, Q., and Zhang, Z.: Large-scale features of Pliocene climate: results from the Pliocene Model Intercomparison Project, *Clim. Past*, 9, 191–209, doi:10.5194/cp-9-191-2013, 2013. 3495

Simulating warmth of the mid-Miocene Climate Optimum in CESM1

A. Goldner et al.

[Title Page](#)

[Abstract](#)

[Introduction](#)

[Conclusions](#)

[References](#)

[Tables](#)

[Figures](#)

[⏪](#)

[⏩](#)

[◀](#)

[▶](#)

[Back](#)

[Close](#)

[Full Screen / Esc](#)

[Printer-friendly Version](#)

[Interactive Discussion](#)

- Henrot, A., Francois, L., Favre, E., Butzin, M., Ouberdous, M., and Munhoven, G.: Effects of CO₂, continental distribution, topography and vegetation changes on the climate at the middle Miocene: A model study, *Clim. Past*, 6, 675–694, doi:10.5194/cp-6-675-2010, 2010. 3491
- Herold, N., Seton, M., Müller, R. D., You, Y., and Huber, M.: Middle Miocene tectonic boundary conditions for use in climate models, *Geochem. Geophys. Geosy.*, 9, Q10009, doi:10.1029/2008GC002046, 2008. 3491
- Herold, N., Huber, M., and Müller, R. D.: Modeling the Miocene Climatic Optimum. Part I: Land and Atmosphere, *J. Climate*, 24, 6353–6372, doi:10.1029/2010PA002041, 2011. 3491, 3500, 3501, 3502
- Herold, N., Huber, M., Müller, R. D., and Seton, M.: Modeling the Miocene climatic optimum: Ocean circulation, *Paleoceanography*, 27, PA1209, doi:10.1029/2010PA002041, 2012. 3493, 3499
- Huber, M.: A hotter greenhouse?, *Science*, 321, 353–354, doi:10.1126/science.1161170, 2008. 3494
- Huber, M. and Caballero, R.: The early Eocene equable climate problem revisited, *Clim. Past*, 7, 603–633, doi:10.5194/cp-7-603-2011, 2011. 3497, 3502
- Hunke, E. C. and Lipscomb, W. H.: CICE: the Los Alamos sea ice model users manual, Version 4, Tech. Report LA-CC-06-012j, Los Alamos National Laboratory, 2008. 3492
- Kay, J. E., Hillman, B., Klein, S., Zhang, Y., Medeiros, B., Gettelman, G., Pincus, R., Eaton, B., Boyle, J., Marchand, R., and Ackerman, T.: Exposing global cloud biases in the Community Atmosphere Model (CAM) using satellite observations and their corresponding instrument simulators, *J. Climate*, 25, 5190–5207, doi:10.1175/JCLI-D-11-00469.1, 2012. 3492
- Kiehl, J. T., Shields, C. A., Hack, J. J., and Collins, W. D.: The climate sensitivity of the Community Climate System Model version 3 (CCSM3), *J. Climate*, 19, 2584–2596, doi:10.1175/JCLI3747.1, 2006. 3501
- Knorr, G., Butzin, M., Micheels, A., and Lohmann, G.: A warm Miocene climate at low atmospheric CO₂ levels, *Geophys. Res. Lett.*, 38, L20701, doi:10.1029/2011GL048873, 2011. 3497, 3501
- Krapp, M. and Jungclaus, J. H.: The Middle Miocene climate as modelled in an atmosphere-ocean-biosphere model, *Clim. Past*, 7, 1169–1188, doi:10.5194/cp-7-1169-2011, 2011. 3491, 3502

Simulating warmth of the mid-Miocene Climate Optimum in CESM1

A. Goldner et al.

[Title Page](#)
[Abstract](#)
[Introduction](#)
[Conclusions](#)
[References](#)
[Tables](#)
[Figures](#)




[Back](#)
[Close](#)
[Full Screen / Esc](#)
[Printer-friendly Version](#)
[Interactive Discussion](#)

- Kürschner, W. M., Kvacek, Z., and Dilcher, D. L.: The impact of Miocene atmospheric carbon dioxide fluctuations on climate and the evolution of terrestrial ecosystems, *Proc. Natl. Acad. Sci.*, 105, 44–453, doi:10.1073/pnas.0708588105, 2008. 3491
- LaRiviere, J. P., Ravelo, A. C., Crimmins, A., Dekens, P. S., Ford, H. L., Lyle, M., and Wara, M. W.: Late Miocene decoupling of oceanic warmth and atmospheric carbon dioxide forcing, *Nature*, 486, 97–100, doi:10.1038/nature11200, 2012. 3491, 3494, 3500
- Lawrence, K. T., Sloan, L. C., and Sewall, J. O.: Terrestrial climatic response to precessional orbital forcing in the Eocene, *Special Papers-Geological Society of America*, 65–78, 2003. 3501
- Lawrence, D. M., Oleson, K. W., Flanner, M. G., Fletcher, C. G., Lawrence, P. J., Levis, S., Swenson, S. C., and Bonan, G. B.: The CCSM4 land simulation, 1850–2005: assessment of surface climate and new capabilities, *J. Climate*, 25, 2240–2260, doi:10.1175/JCLI-D-11-00103.1, 2012. 3492
- Lunt, D. J., Dunkley Jones, T., Heinemann, M., Huber, M., LeGrande, A., Winguth, A., Loptson, C., Marotzke, J., Roberts, C. D., Tindall, J., Valdes, P., and Winguth, C.: A model – data comparison for a multi-model ensemble of early Eocene atmosphere – ocean simulations: EoMIP, *Clim. Past*, 8, 1717–1736, doi:10.5194/cp-8-1717-2012, 2012. 3497
- Lyle, M., Barron, J., Bralower J., Huber, M., Lyle, A. O., Ravelo, A. C., Rea, R. K., and Wilson, P.: Pacific Ocean and cenozoic evolution of climate, *Rev. Geophys.*, 46, RG2002, doi:10.1029/2005RG000190, 2008. 3499
- Molnar, P. and Cane, M. A.: Early Pliocene (pre–Ice Age) El Niño like global climate: which El Niño?, *Geosphere*, 3, 337–365, doi:10.1130/?GES00103.1, 2007. 3499
- Mosbrugger, V. and Utescher, T.: The coexistence approach a method for quantitative reconstructions of Tertiary terrestrial palaeoclimate data using plant fossils, *Palaeogeogr. Palaeocli.*, 134, 61–86, doi.org/10.1016/S0031-0182(96)00154-X, 1997. 3494
- Müller, R. D., Sdrolias, M., Gaina, C., Steinberger, B., and Heine, C.: Long-term sea-level fluctuations driven by ocean basin dynamics, *Science*, 319, 1357–1362, doi:10.1126/science.1151540, 2008.
- Neale, R. B., Richter, J., Park, S., Lauritzen, P. H., Vavrus, S. J., Rasch, P. J., and Zhang, M.: The mean climate of the community atmosphere model (CAM4) in forced SST and fully coupled experiments, *J. Climate*, doi:10.1175/JCLI-D-12-00236.1, in press, 2013. 3492

Simulating warmth of the mid-Miocene Climate Optimum in CESM1

A. Goldner et al.

[Title Page](#)[Abstract](#)[Introduction](#)[Conclusions](#)[References](#)[Tables](#)[Figures](#)[⏪](#)[⏩](#)[◀](#)[▶](#)[Back](#)[Close](#)[Full Screen / Esc](#)[Printer-friendly Version](#)[Interactive Discussion](#)

- Nikolaev, S. D., Oskina, N. S., Blyum, N. S., and Bubenshchikova, N. V.: Neogene-Quaternary variations of the “pole-equator” temperature gradient of the surface oceanic waters in the North Atlantic and North Pacific, *Global Planet. Change*, 18, 85–111, 1998. 3491
- Pagani, M.: The alkenone- CO_2 proxy and ancient atmospheric carbon dioxide, *Philos. T. Roy. Soc. A*, 360, 609–632, doi:10.1098/rsta.2001.0959, 2002. 3492
- Pagani, M., Zachos, J. C., Freeman, K. H., Tiplle, B., and Bohaty, S.: Marked decline in atmospheric carbon dioxide concentrations during the Paleogene, *Science*, 309, 600–603, doi:10.1126/science.1110063, 2005. 3491
- Pearson, P. N. and Palmer, M. R.: Atmospheric carbon dioxide concentrations over the past 60 million years, *Nature* 406, 695–699, doi:10.1038/35021000, 2000. 3491, 3492
- Pekar, S. F. and DeConto, R. M.: High-resolution ice-volume estimates for the early Miocene: evidence for a dynamic ice sheet in Antarctica, *Palaeogeogr. Palaeocli.*, 231, 101–109, doi:10.1016/j.palaeo.2005.07.027, 2006. 3498
- Philander, S. G. and Fedorov, A. V.: Role of tropics in changing the response to Milankovitch forcing some three million years ago, *Paleoceanography*, 18, 1045, doi:10.1029/2002PA000837, 2003. 3499
- Potter, P. E. and Sztamari, P.: Global Miocene tectonics and the modern world, *Earth-Sci. Rev.*, 96, 279–295, doi:10.1016/j.earscirev.2009.07.003, 2009. 3492
- Pound, M., Haywood, A. M., Salzman, U., and Riding J. B.: Global vegetation dynamics and latitudinal temperature gradients during the Mid to LateMiocene (15.97–5.33Ma), *Earth-Sci. Rev.*, 112, 1–22, doi:10.1016/j.earscirev.2012.02.005, 2012. 3490
- Ravelo, A. C., Dekens, P. S., and McCarthy, M.: Evidence for El Niño like conditions during the Pliocene, *GSA Today*, 16, 4–11, 2006. 3494, 3499
- Royer, D. L.: Climate reconstruction from leaf size and shape: new developments and challenges, in: *Reconstructing Earth’s Deep-Time Climate – The State of the Art in 2012*, edited by: Ivany, L. C. and Huber, B. T., *Paleontological Society Papers*, 18, 195–212 (invited contribution), 2012. 3494
- Royer, D. L., Osborne, C. P., and Beerling, D. J.: High CO_2 increases the freezing sensitivity of plants: Implications for paleoclimatic reconstructions from fossil floras, *Geology*, 30, 963–966, doi:10.1130/0091-7618(2002)030<0963:HCITFS>2.0.CO;2, 2002. 3492
- Savin, S. M.: The history of the Earth’s surface temperature during the past 100 million years, *Annu. Rev. Earth Planet. Sci.*, 5, 319–355, 1977. 3491

Simulating warmth of the mid-Miocene Climate Optimum in CESM1

A. Goldner et al.

[Title Page](#)

[Abstract](#)

[Introduction](#)

[Conclusions](#)

[References](#)

[Tables](#)

[Figures](#)

[⏪](#)

[⏩](#)

[◀](#)

[▶](#)

[Back](#)

[Close](#)

[Full Screen / Esc](#)

[Printer-friendly Version](#)

[Interactive Discussion](#)

- Sexton, P., Wilson, P., Pearson, P.: Microstructural and geochemical perspectives on planktic foraminiferal preservation: “glassy” versus “frosty”, *Geochem. Geophys. Geosyst.*, 7, Q12P19, doi:10.1029/2006GC001291, 2006. 3494
- Shevenell, A. E., Kennett, J. P., and Lea, D. W.: Middle Miocene southern ocean cooling and Antarctic cryosphere expansion, *Science*, 305, 1766–1770, doi:10.1126/science.1100061, 2004. 3491
- Shevenell, A. E., Kennett, J. P., and Lea, D. W.: Middle Miocene ice sheet dynamics, deep-sea temperatures, and carbon cycling: A Southern Ocean perspective, *Geochem. Geophys. Geosyst.*, 9, Q02006, doi:10.1029/2007GC001736, 2008. 3491, 3498
- Shields, C. A., Bailey, D. A., Danabasoglu, G., Jochum, M., Kiehl, J. T., Levis, S., and Park, S.: The Low-Resolution CCSM4, *J. Climate*, 25, 3993–4014, doi:10.1175/JCLI-D-11-00260.1, 2012. 3499
- Sloan, L. C. and Huber, M.: Eocene oceanic responses to orbital forcing on precessional time scales, *Paleoceanography*, 16, 101–111, doi:10.1029/1999PA000491, 2001. 3501
- Striver, L. and Huber, M.: Modeled sensitivity of upper thermocline properties to tropical cyclone winds and possible feedbacks on the Hadley circulation, *Geophys. Res. Lett.*, 37, L08704, doi:doi:10.1029/2010GL042836, 2010. 3500
- Stewart, D. R. M., Pearson, P. N., Ditchfield, P. W., and Singano, J. M.: Miocene tropical Indian Ocean temperatures: Evidence from three exceptionally preserved foraminiferal assemblages from Tanzania, *J. Afr. Earth Sci.*, 40, 173–189, doi:10.1016/j.jafrearsci.2004.09.001, 2004. 3491
- Tang, H., Eronen, J. T., Micheels, A., and Ahrens, B. Strong interannual variation of the Indian summer monsoon in the Late Miocene, *Clim. Dynam.*, doi:10.1007/s00382-012-1655-y, in press, 2013. 3499
- Tong, J. A., You, Y., Müller, R. D., and Seton, M.: Climate model sensitivity to atmospheric CO₂ concentrations for the middle Miocene, *Global Planet. Change*, 67, 129–140, doi:10.1016/j.gloplacha.2009.02.001, 2009. 3491, 3493
- Vizcaíno, M., Rupper, S., and Chiang, J. C. H.: Permanent El Niño and the onset of Northern Hemisphere glaciations: mechanism and comparison with other hypotheses, *Paleoceanography*, 25, PA2205, doi:10.1029/2009PA001733, 2010. 3499
- Wang, S. Y., L’Heureux, M., and Yoon, J. H.: Are greenhouse gases changing ENSO precursors in the Western North Pacific?, *J. Climate*, doi:10.1175/JCLI-D-12-00360.1, online first, 2013. 3499

**Simulating warmth of
the mid-Miocene
Climate Optimum in
CESM1**A. Goldner et al.

[Title Page](#)[Abstract](#)[Introduction](#)[Conclusions](#)[References](#)[Tables](#)[Figures](#)[⏪](#)[⏩](#)[◀](#)[▶](#)[Back](#)[Close](#)[Full Screen / Esc](#)[Printer-friendly Version](#)[Interactive Discussion](#)

- Westerhold, T., Bickert, T., and Röhl, U.: Middle to late Miocene oxygen isotope stratigraphy of ODP site 1085 (SE Atlantic): new constrains on Miocene climate variability and sea-level fluctuations, *Palaeogeogr. Palaeocli.*, 217, 205–222, 2005. 3501
- 5 You, Y., Huber, M., Mueller, D., Poulsen, C. J., and Ribbe, J.: Simulation of the Middle Miocene climate optimum, *Geophys. Res. Lett.*, 36, L04702, doi:10.1029/2008GL036571, 2009. 3491, 3493
- Zachos, J. C., Dickens, G. R., and Zeebe, R. E.: An early Cenozoic perspective on greenhouse warming and carbon-cycle dynamics, *Nature*, 451, 279–283, doi:10.1038/nature06588, 2008. 3490
- 10 Zhang, Y. G., Pagani, M., Liu, Z., Bohaty, M., and DeConto, R.: A 40-million-year history of atmospheric CO₂, *Phil. Trans. R. Soc. A*, in press, 2013. 3491

Simulating warmth of the mid-Miocene Climate Optimum in CESM1

A. Goldner et al.

[Title Page](#)[Abstract](#)[Introduction](#)[Conclusions](#)[References](#)[Tables](#)[Figures](#)[⏪](#)[⏩](#)[◀](#)[▶](#)[Back](#)[Close](#)[Full Screen / Esc](#)[Printer-friendly Version](#)[Interactive Discussion](#)

Table 1. Compilation of model and proxy MAT values, equator to pole temperature gradient values, and model data point wise comparison statistics.

Simulation Name and Records	MAT (°C)	Miocene minus PI (°C)	Equator to Pole Temperature Gradient (°C) ^a	Slope ^b	Y-intercept of best fit line ^b	RMS Error
MMCO Records	21.89 ± 2.2	–	24.50	–	–	–
PI	13.95	–	43.84	1.29	–13.73	10.12
PI400	15.57	1.62	42.16	–	–	–
MMCO	18.00	4.04	41.79	1.11	–5.91	6.05
MMCO560	19.84	5.89	37.50	1.09	–2.39	5.72
MMCO800	21.19	7.26	33.00	0.95	–0.21	4.81
LOW AIS	18.10	4.15	39.08	1.01	–5.54	5.23
EP	18.68	4.66	37.89	1.08	–5.32	5.99
EP+ORB	19.66	5.64	33.79	1.06	–3.86	5.19
CCSM3.0 T31						
355 ppm CO ₂	15.38	1.43	37.00	–	–	–
CCSM3.0 T31						
560 ppm CO ₂	16.94	2.99	35.00	–	–	–

^a The equator to pole surface temperature gradient is calculated by averaging the mean annual temperatures over the absolute latitudes of (60–80°) minus (0–30°); 80° is the maximum latitudinal extent of proxy records. ^b The slope and y-intercept of the best fit line for the pointwise model and proxy comparisons in Figs. 2, 3, 4, 5, 6. The best fit line is weighted to include the error uncertainty found in the proxy records (Tables S1, S2).

Simulating warmth of the mid-Miocene Climate Optimum in CESM1

A. Goldner et al.

Table 2. High latitude model proxy data comparison for the Alaskan and Antarctic records. The simulations in the comparison include CESM1.0 and CCSM3.0 (Herold et al., 2011) model runs.

	Latitude (°)	Proxy (°C)	Error (±°C)	MMCO (°C)	MMCO 560	LOW AIS	EP	EP+ ORBI TAL25	CCSM3.0 T31 355 ppm CO ₂	PI
Porcupine River 90-1, Organic bed	68.19° N	8.00	8.00	-7.00	-3.7	-7.40	-5.20	-3.0	-6.80	-10.81
Nenana Coal Fm	65.11° N	7.50	8.00	0.00	2.9	-0.50	1.30	3.20	-5.59	-10.35
Coal Creek	64.99° N	8.00	8.00	0.00	2.9	-0.50	1.30	3.20	-5.59	-10.35
Cook Inlet	62.00° N	11.00	3.00	2.10	4.60	1.30	3.10	4.90	1.39	-9.95
AND-2A (Ross Sea)	-77.00° S	5.50	5.00	-1.50	0.00	-1.43	-1.40	-0.25	-1.72	-1.73

[Title Page](#)[Abstract](#)[Introduction](#)[Conclusions](#)[References](#)[Tables](#)[Figures](#)[⏪](#)[⏩](#)[◀](#)[▶](#)[Back](#)[Close](#)[Full Screen / Esc](#)[Printer-friendly Version](#)[Interactive Discussion](#)

Simulating warmth of the mid-Miocene Climate Optimum in CESM1

A. Goldner et al.

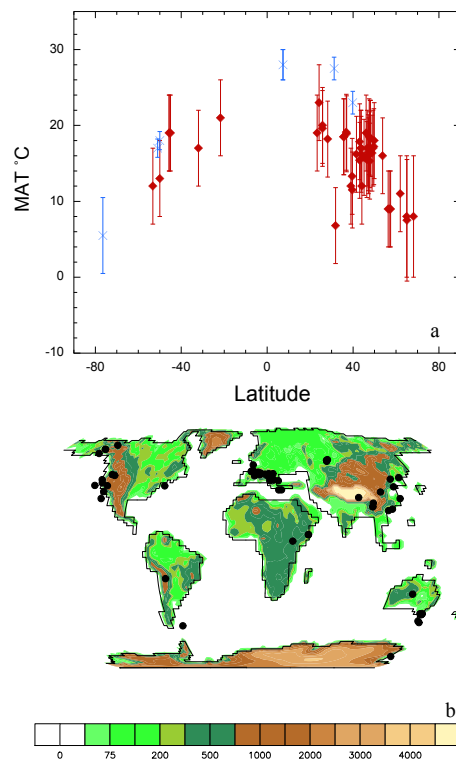


Fig. 1. (a) Longitudinal distribution of MMCO terrestrial temperatures (red diamonds) and SST (blue crosses) with proxy record error plotted as the vertical bars and described in Tables S1 and S2. **(b)** The spatial distribution of the terrestrial and SST proxy records used in the model data comparisons overlay onto the Miocene topography (Herold et al., 2008).

Simulating warmth of the mid-Miocene Climate Optimum in CESM1

A. Goldner et al.

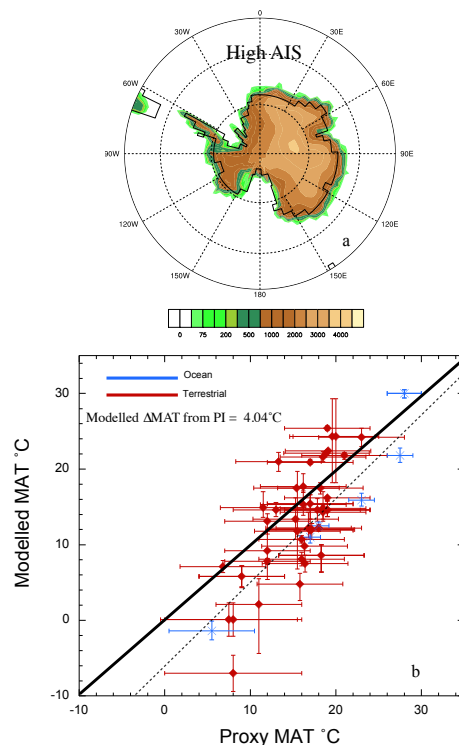


Fig. 2. (a) High AIS topography used in Herold et al. (2011), (b) Pointwise MAT comparison between the MMCO simulation and proxy records (Tables S1 and S2). Vertical error bars are the modelled pointwise maximum and minimum temperatures from the extreme obliquity simulations (see Methods Sect. 2.3) and methodological error is plotted as the horizontal error bars. The best fit line (black dashed) is weighted to include proxy uncertainty and is fitted across all points. The weighting for each proxy record is calculated by $1/(\text{error}^2)$. The y-intercept and slope are reported in Table 1.

[Title Page](#)
[Abstract](#)
[Introduction](#)
[Conclusions](#)
[References](#)
[Tables](#)
[Figures](#)
[⏪](#)
[⏩](#)
[◀](#)
[▶](#)
[Back](#)
[Close](#)
[Full Screen / Esc](#)
[Printer-friendly Version](#)
[Interactive Discussion](#)

Simulating warmth of the mid-Miocene Climate Optimum in CESM1

A. Goldner et al.

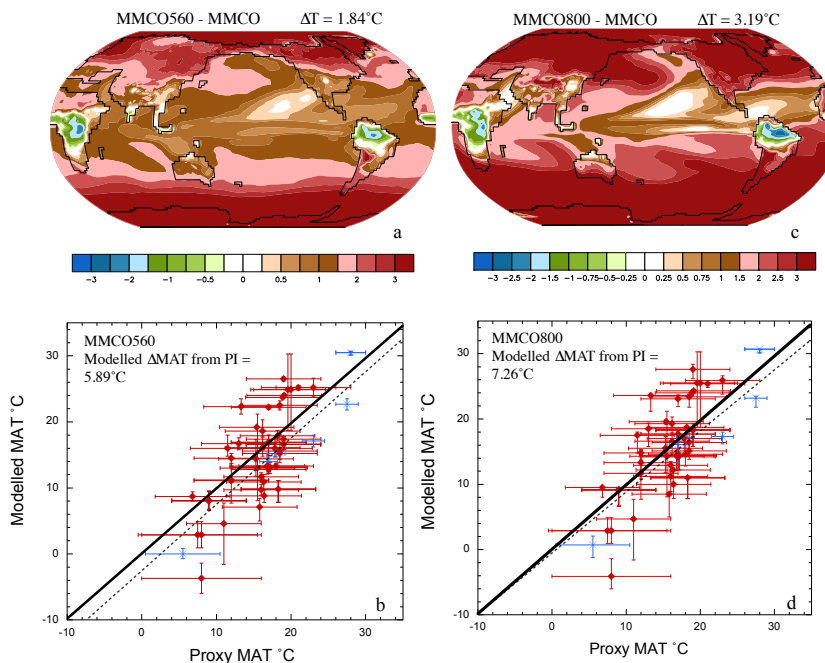


Fig. 3. (a) Modelled temperature anomaly for the MMCO560 (560 ppm CO₂) simulation minus the MMCO simulation ($^\circ\text{C}$). (b) Pointwise MMCO560 simulated global MAT compared against the proxy record MAT ($^\circ\text{C}$). (c) Modelled temperature anomaly for the MMCO800 (800 ppm CO₂) simulation minus the MMCO simulation ($^\circ\text{C}$). (d) Pointwise MMCO800 simulated global MAT compared against the proxy record MAT ($^\circ\text{C}$). These are the same terrestrial and SST records described in Fig. 1. Vertical error bars indicate the uncertainty recorded by maximum and minimum temperatures of extreme orbital obliquity parameters (see Methods Sect. 2.3). The best fit line (black dashed) is weighted to include error uncertainty is fitted across all points and the y-intercept and slope reported in Table 1

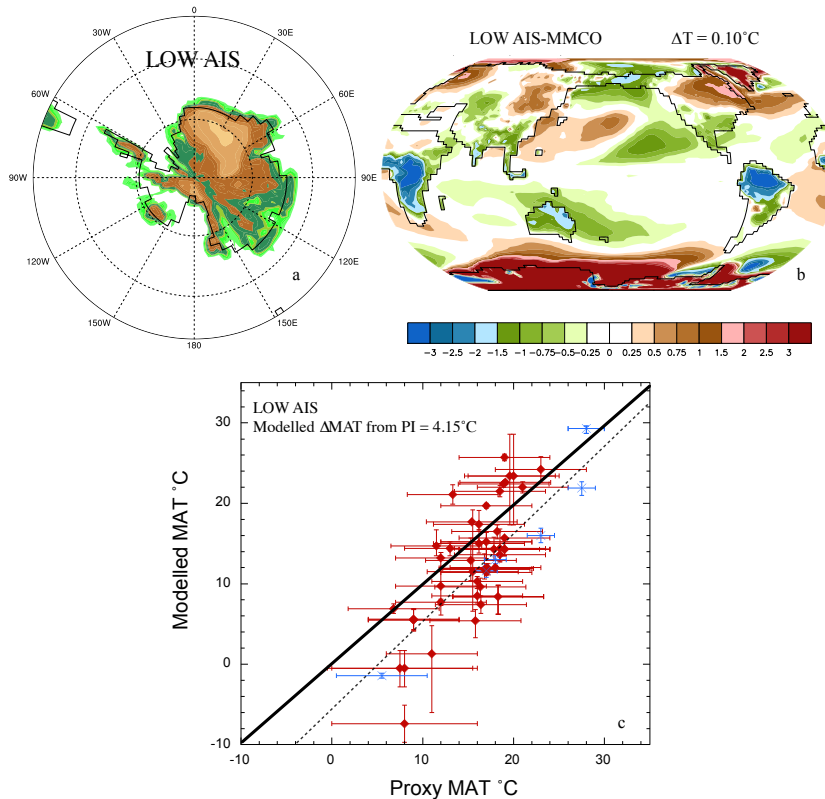


Fig. 4. (a) LOW AIS topography based on offline ice-sheet modeling (David Pollard, personal comms), (b) modelled temperature anomaly ($^\circ\text{C}$) between the LOW AIS simulation and the MMCO simulation with the high AIS. (c) Pointwise MAT comparison between the LOW AIS simulation and proxy records (Tables S1 and S2). The best fit line (black dashed) is weighted to include error uncertainty and is fitted across all points and the y-intercept and slope are reported in Table 1.

Simulating warmth of the mid-Miocene Climate Optimum in CESM1

A. Goldner et al.

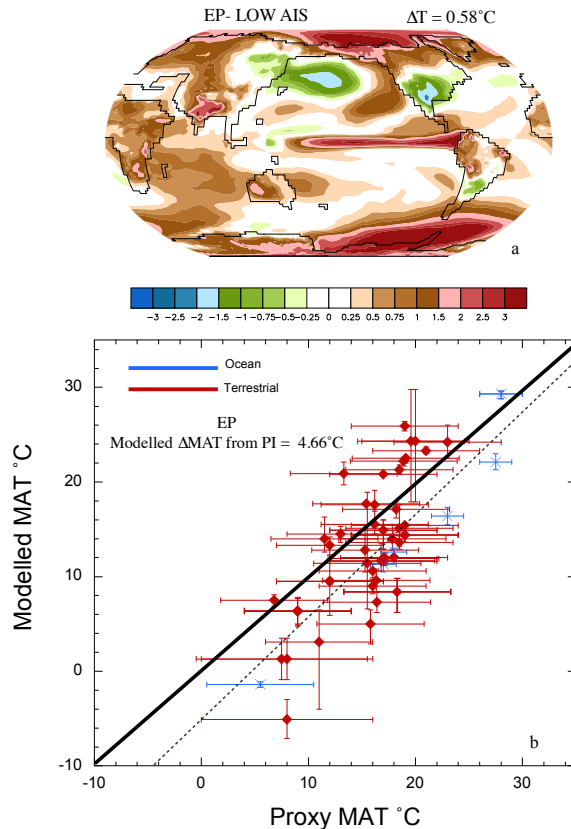


Fig. 5. (a) Modelled temperature anomaly for the EP simulation minus the LOW AIS simulation ($^\circ\text{C}$), (b) Pointwise EP case global mean MAT compared against the proxy record MAT ($^\circ\text{C}$). These are the same terrestrial and SST records and error bars described in Fig. 1. The best fit line (black dashed) is weighted to include error uncertainty and is fitted across all points and the y-intercept and slope reported in Table 1.

Title Page

Abstract

Introduction

Conclusions

References

Tables

Figures

⏪

⏩

◀

▶

Back

Close

Full Screen / Esc

Printer-friendly Version

Interactive Discussion

Simulating warmth of the mid-Miocene Climate Optimum in CESM1

A. Goldner et al.

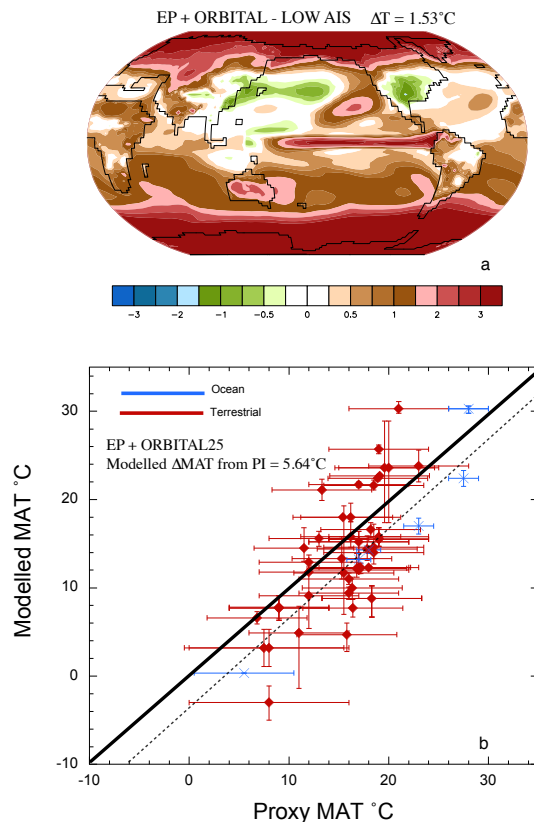


Fig. 6. (a) Modelled temperature anomaly for the EP+ORBITAL25 simulation minus the LOW AIS simulation ($^\circ\text{C}$), (b) Pointwise EP+ORBITAL25 case global mean MAT compared against the proxy record MAT ($^\circ\text{C}$). These are the same terrestrial and SST records described in Fig. 1. Vertical error bars indicate the uncertainty recorded by maximum and minimum temperatures of extreme orbital obliquity same as Fig. 1. The best fit line (black dashed) is weighted to include error uncertainty is fitted across all points and the y-intercept and slope reported in Table 1.

Title Page

Abstract

Introduction

Conclusions

References

Tables

Figures

◀

▶

◀

▶

Back

Close

Full Screen / Esc

Printer-friendly Version

Interactive Discussion